Crystal Structure, Matrix-Isolation FTIR, and UV-Induced Conformational Isomerization of 3-Quinolinecarboxaldehyde

ARTICLE *in* THE JOURNAL OF PHYSICAL CHEMISTRY A · AUGUST 2014

Impact Factor: 2.69 · DOI: 10.1021/jp506354t · Source: PubMed

THE JOURNAL OF PHYSICAL CHEMISTRY A

Article

pubs.acs.org/JPCA

Crystal Structure, Matrix-Isolation FTIR, and UV-Induced Conformational Isomerization of 3-Quinolinecarboxaldehyde

Nihal Kuş,*[,†,‡] Marta Sofia Henriques,[§] José António Paixão,[§] Leszek Lapinski,[†,∥] and Rui Fausto[†]

[†]CQC, Department of Chemistry, University of Coimbra, 3004-535 Coimbra, Portugal

[‡]Department of Physics, Anadolu University, 26470 Eskişehir, Turkey

[§]CEMDRX, Department of Physics, University of Coimbra, 3004-516 Coimbra, Portugal

[∥]Institute of Physics, Polish Academy of Sciences, Al. Lotnikow 32/46, 02-668 Warsaw, Poland

Supporting Information

ABSTRACT: The crystal structure of 3-quinolinecarboxaldehyde (3QC) has been solved, and the compound has been shown to crystallize in the space group $P2_1/c$ (monoclinic) with a = 6.306(4), b = 18.551(11), c = 6.999(4) Å, β = 106.111(13)°, and Z = 4. The crystals were found to exhibit pseudomerohedral twinning with a twin law corresponding to a two-fold rotation around the monoclinic (100) reciprocal lattice axis (or [4 0 1] in direct space). Individual molecules adopt the syn conformation in the crystal, with the oxygen atom of the aldehyde substituent directed toward the same side of the ring nitrogen atom. In the gas phase, the compound exists in two nearly isoenergetic conformers (syn and anti), which could be successfully trapped in solid argon at 10 K, and their infrared spectra are registered and interpreted. Upon in situ irradiation of matrix-isolated 3QC with UV light (λ > 315 nm), significant reduction of the population of the less stable anti conformer was observed, while that of the conformational ground state (syn conformer) increased, indicating occurrence of the anti → syn isomerization. Upon irradiation at higher energy (λ > 235 nm), the syn → anti reverse photoreaction was observed. Interpretation of the structural, spectroscopic, and photochemical experimental data received support from quantum chemical theoretical results obtained at both DFT/B3LYP (including TD-DFT investigation of excited states) and MP2 levels, using the 6-311++G(d,p) basis set.

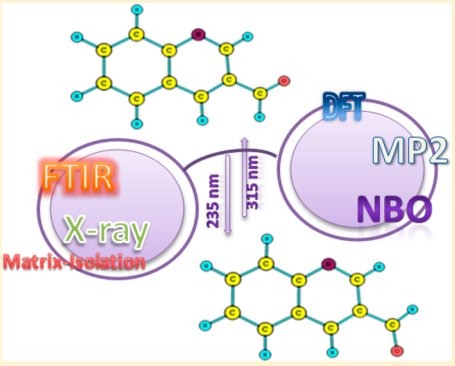

INTRODUCTION

Quinolines are a class of heteroaromatic organic compounds characterized by a double-ring structure composed of a benzene and a pyridine ring fused at two adjacent carbon atoms. The parent quinoline (C_9H_7N) has been known since 1834 and was isolated first by Friedlieb F. Runge, the German analytical chemist who also identified caffeine.[1] Quinoline is used as a precursor to 8-hydroxyquinoline, which is a versatile chelating agent and precursor to pesticides.[2] Compounds containing the quinoline motif show a broad range of applications. Probably the most known quinoline derivative is quinine, widely used as first-line antimalarial in the past (and still used presently when artemisinins are not available).[3,4] Quinoline derivatives are also used as antibacterial[5] and anticancer agents,[6] and find additional uses, for example, in the synthesis of fungicides, virucides, biocides, alkaloids, rubber chemicals, and flavoring agents.[7,8]

The quinolinecarboxaldehydes have also been found to exhibit relevant biological properties, in particular, antimicrobial activity.[9−16] From a more fundamental perspective, they have been reported to present interesting physicochemical properties, which have mostly been assigned to the presence of the conformationally flexible aldehyde substituent and, in the solid state, also to the presence of weak $\pi\cdots\pi$ and C−H$\cdots\pi$ contacts and C−H···O hydrogen-bond-type intermolecular interactions.[17−22] For isolated molecules, the intramolecular degree of freedom associated with internal rotation of the aldehyde substituent plays the major role in determining conformationally related properties of such compounds.

The present investigation focused on 3-quinolinecarboxaldehyde (3QC). Such as found for other aromatic aldehydes,[23−25] the isolated molecule of 3QC could be expected to possess two low-energy conformers differing in the orientation of the aldehyde group (syn and anti; Scheme 1). As will be described in detail below, we succeeded in trapping the two conformers of 3QC in solid argon at 10 K as well as in promoting their controlled interconversion by applying in situ UV light of different energies. A detailed assignment of the infrared spectra of the two conformers observed in the low-temperature matrixes is presented, which is also supported by normal coordinate analysis. In addition, the crystal structure of 3CQ was solved using X-ray diffraction, and the crystal was shown to exhibit an interesting pseudomerohedral twinning with molecules adopting the syn conformation.

Received: June 26, 2014
Revised: August 19, 2014

   dx.doi.org/10.1021/jp506354t | J. Phys. Chem. A XXXX, XXX, XXX−XXX

Scheme 1. Conformers of 3QC

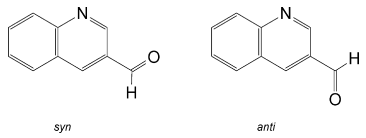

EXPERIMENTAL AND COMPUTATIONAL METHODS

Matrix Isolation FTIR and Photochemical Experiments. A commercial sample of 3QC (Aldrich, 98%) was used without any further purification. The vapor of the compound at room temperature was co-deposited together with a large excess of the host matrix gas (argon N60, Air Liquide) onto a cold CsI window (T = 10 K) mounted on the tip of the cryostat. The compound was sublimated in a specially designed Knudsen cell with shut-off possibility, whose main component is a NUPRO SS-4BMRG needle valve. All experiments were done on the basis of an APD Cryogenics closed-cycle helium refrigeration system with a DE-202A expander. Infrared spectra were obtained using a Mattson (Infinity 60AR Series) Fourier transform infrared (FTIR) spectrometer equipped with a deuterated triglycine sulfate (DTGS) detector and a Ge/KBr beam splitter, with 0.5 cm^{-1} spectral resolution. To avoid interferences from H_2O and CO_2, a flux of air free of water vapor and carbon dioxide continuously purged the optical path of the spectrometer. The matrixes were irradiated through the outer quartz window of the cryostat, using a 500 W Hg(Xe) lamp (Oriel, Newport) set up to provide a 200 W output power, combined with long-pass filters with cutoff wavelengths of 315 and 235 nm.

X-ray Studies. Data collection was performed on a Bruker APEXII diffractometer with Mo Kα radiation (λ = 0.71073 Å). The crystals were found to be twinned, with a diffraction pattern that is metrically orthorhombic. Data collection was performed on the pseudo-orthorhombic C-centered cell with a = 7.0018(3), b = 24.2376(10), and c = 18.5563(7) Å. The large R_{int} = 0.15 for equivalent reflections in the orthorhombic Laue group of lower symmetry pointed out to a twinned crystal, and indeed, the structure could not be properly solved and refined in an orthorhombic space group. The structure was solved in space group $P1$ using direct methods, and the correct symmetry was subsequently found to be monoclinic and space group $P2_1/c$ with a = 6.306(4), b = 18.551(11), c = 6.999(4) Å, and β = 106.111(13)°. Analysis of the data with PLATON confirmed the presence of pseudomerohedral twinning with a twin law corresponding to a two-fold rotation around the monoclinic (100) reciprocal lattice axis (or [4 0 1] in direct space). Refinement of the structure using such a twin law and the SHELXL-97 BASF and HKLF5 instructions gave a final R_1 factor of 0.0547 (for 929 reflections with $I > 2\sigma(I)$) and R_{all} = 0.1384 for all 1942 data and 111 parameters (full anisotropic model, with H atoms riding on their parent atoms). The X-ray analysis shows that the molecule adopts a syn conformation in the crystal (Figure 1). Bond lengths and angles are within typical values. Crystal data and details of the structure determination are provided in Tables S1–S6 and Figure S1 in the Supporting Information. The crystal structure has been deposited at the Cambridge Crystallographic Data Centre (deposition number CCDC 1010325). XRD data collection on a polycrystalline sample was performed to check the homogeneity of our sample and the unique presence of the structure found in the single-crystal work. Data were collected on a Bruker D8 Advance diffractometer in Bragg–Brentano geometry using Ni-filtered Cu Kα radiation (λ = 1.54056 Å). A Rietveld refinement using the TOPAS program fitted all of the peaks, showing that no variants of the described crystal structure exist in the polycrystalline sample (Figure S2, Supporting Information).

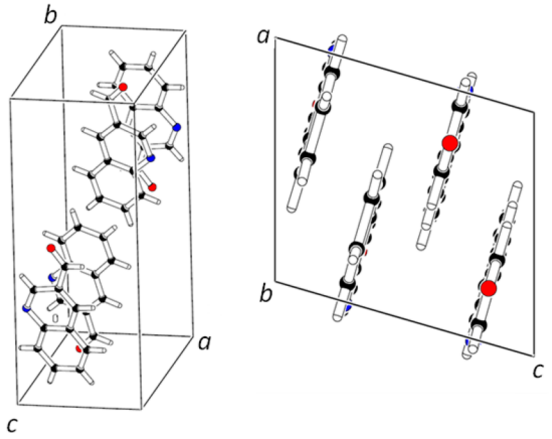

Figure 1. Two views of the unit cell of the crystal structure of 3QC. Axes a, b, and c are indicated; the right view is along the b axis.

Theoretical Calculations. The quantum chemical calculations were carried out using the Gaussian 09 program.[26] Optimized geometries, energies, and infrared frequencies and intensities were obtained at the DFT level of approximation using the 6-311++G(d,p) basis set[27] and the B3LYP functional, which uses the Becke's three-parameter exchange functional[28] and the Lee, Yang, and Parr[29] and Vosko, Wilk, and Nusair[30] correlation functionals. Transformations of the Cartesian force constants to molecule-fixed symmetry-adjusted internal coordinates allowed the ordinary normal coordinate analysis to be performed as described by Schachtschneider and Mortimer.[31] Natural bond orbital (NBO) analysis was performed according to Weinhold and co-workers[32,33] using NBO 3.1, as implemented in Gaussian 09. Energies of the low-energy excited states were calculated using time-dependent density functional theory (TD-DFT)[34,35] at the B3LYP/6-311++G(d,p) level.

RESULTS AND DISCUSSION

Theoretical Study of the Conformational Isomerism in 3QC. A theoretical study of 3QC has been reported before by Kumru et al.[36] Very unfortunately, in that study, some important results were not reported correctly. For example, it is stated in the cited article that conformer anti of 3QC has been predicted by DFT(B3LYP)/6-311++G(d,p) calculations to be "more stable than conformer syn by ~6 kcal mol^{-1}" (i.e., ~25 kJ mol^{-1})[36] and that zero-point vibrational corrections to the energy "do not contribute much to the relative stabilities of the two conformers".[36] In fact, the DFT(B3LYP)/6-311++G(d,p) calculations predict the two conformers to be nearly isoenergetic, with the anti conformer being only 0.041 kJ mol^{-1} lower in energy than the syn form. In addition, according to the calculations, zero-point corrections are important enough to reverse the relative order of energy of the conformers, with the anti form having a zero-point-corrected energy slightly larger than that from the syn form by 0.037 kJ mol^{-1}. Taking temperature (298 K) into account, leads to prediction [at the

dx.doi.org/10.1021/jp506354t | J. Phys. Chem. A XXXX, XXX, XXX–XXX

DFT(B3LYP)/6-311++G(d,p) level] of the relative Gibbs energies of the conformers differing by 0.073 kJ mol^{-1}, in favor of higher stability of the syn form. At the MP2 level of approximation (with the same basis set; more reliable for energy predictions), the syn form has been calculated in the present investigation to be lower in energy than the anti form by 0.31 kJ mol^{-1} (1.17 kJ mol^{-1}, after consideration of zero-point energy). At this level of theory, the Gibbs energy difference (at 298 K) favors also the syn conformer by 1.44 kJ mol^{-1}. It can then be concluded that the syn conformer of 3QC shall in fact be slightly more stable than the anti conformer of the compound. Consequently, in the gas phase at 298 K, the syn conformer should be somewhat more populated than the anti form. Note that a similar trend has been observed for 6-quinolinecarboxaldehyde (6QC), where the syn conformer was also found to be slightly more stable than the anti form.[20] In both 3QC and 6QC, the proximal environment of the aldehyde group is identical in the two conformers, and the polarity of the syn form is larger than that of the anti form (ca. 4.5 versus 2.5 D). In contrast, for 2-quinolinecarboxaldehyde,[19] the anti conformer corresponds to the most stable form because in this molecule, the anti structure is stabilized by the attractive interaction between the nearly antiparallelly aligned bond dipoles associated with the vicinal aldehyde C−H and ring CN bonds.

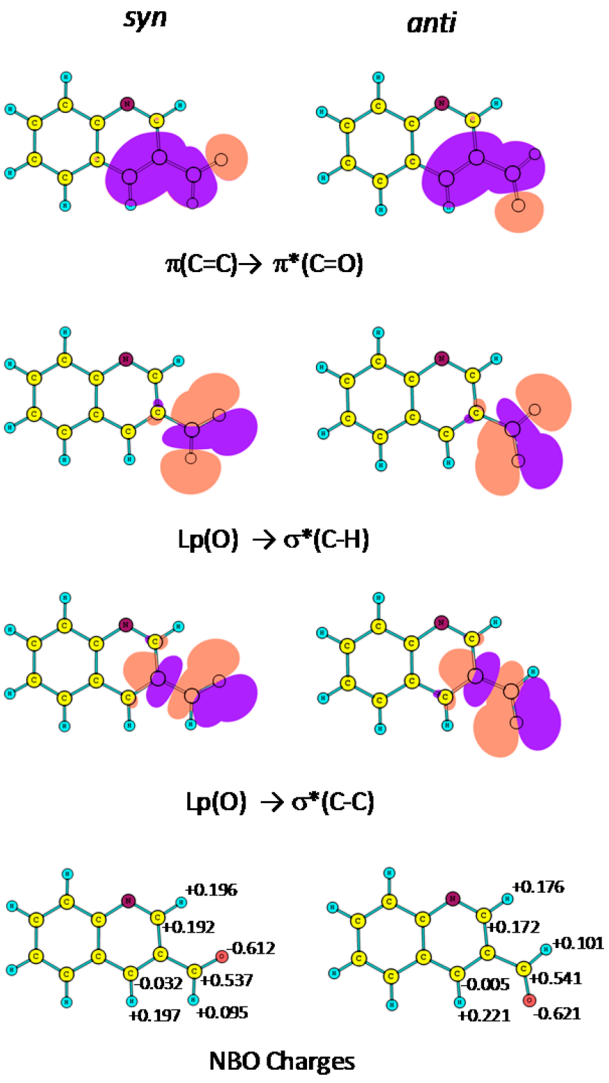

Figure 2. Electron density surfaces (isovalues of the electron densities equal to 0.03 *e*) showing selected NBO interactions for syn and anti conformers of 3QC (top) and NBO charges (units of *e*) on selected atoms (bottom). In the calculations, the MP2/6-311++G(d,p) wave functions were used; the complete list of NBO charges is provided in Table S7 (Supporting Information).

Considering the structural similarity of the two conformers of 3QC (see Table S5 (Supporting Information) for geometries), their relative stability must be determined by subtle factors. In order to shed light on this question, we performed the NBO analysis of the two forms, using the corresponding calculated MP2/6-311++G(d,p) wave functions. Such analysis allows to identify the main orbital interactions resulting from the second-order perturbation theory analysis of the Fock matrix.[32,33] In addition, we have also calculated the NBO charges and used them to extract relevant information regarding the differences in the intramolecular effects in the two conformers resulting from interactions between the bond dipoles involving the aldehyde group (associated with the aldehyde C−H and C═O bonds) and the vicinal C−H bonds of the ring system. The results are summarized in Figure 2 (see also Table S7 in the Supporting Information).

Besides the NBO interactions expressing the electronic delocalization within the rings (which are identical in the two conformers), the most important orbital interactions (see Figure 2) occur (i) between the vicinal to the aldehyde group π(C═C) orbital, which in the syn conformer is eclipsed with the C−H aldehyde bond and in the anti conformer eclipses the C═O bond as the donor, and the π(C═O)* antiligand orbital as the acceptor and (ii) between the σ-system p-type lone-electron pair orbital of the O atom (Lp(O); donor) (according to the NBO calculations, the carbonyl oxygen atom is sp-hybridized, with one of the two hybrid orbitals forming the σ(C═O) bond and the other being occupied by a lone pair of electrons, while the two p orbitals form the π(C═O) bond and accommodate the second lone electron pair) and the exocyclic σ(C−C)* and aldehyde σ(C−H)* orbitals (acceptors). Interaction (i) directly couples the aldehyde C═O bond with the ring system, expressing the degree of delocalization of the π-system of the molecule into the aldehyde fragment. The geometry of interaction is different in the two conformers, and as could be expected,[37,38] this interaction is more efficient for the anti-periplanar arrangement of the interacting C═C−C═O fragment occurring in the syn conformer of 3QC than for the syn-periplanar arrangement of this fragment found in the anti conformer (see Figure 2). According to the calculations, this distinctive stabilizing interaction is stronger in the syn conformer than that in the anti form by ∼8 kJ mol^{-1}. Interactions of type (ii) relate with the well-known charge back-donnation effect that was described long ago as the most important effect leading to the observed elongation of a C−H bond connected to a carbonyl moiety as well as to its reduced C−H stretching frequency (e.g., in aldehydes and formic acid derivatives).[39−41] Orbital interactions (ii) were also found to be more important in syn than in anti 3QC, with the Lp(O) → σ*(C−H) and Lp(O) → σ*(C−C) stabilizing more the syn conformer than the anti form by 5 and 2 kJ mol^{-1}, respectively. On the whole, orbital interactions (i) and (ii) favor the syn conformer by ∼15 kJ mol^{-1}.

On the other hand, the charge interactions between the bond dipoles involving the aldehyde group (associated with the aldehyde C−H and C═O bonds) and the vicinal C−H bonds

dx.doi.org/10.1021/jp506354t | J. Phys. Chem. A XXXX, XXX, XXX−XXX

of the ring system favor the anti conformer of 3QC (see Figure 2). Indeed, while in the anti conformer the most relevant bond dipole interaction involving the highly polarized C═O bond is established with a C−H ring bond that also shows a considerable degree of polarization, in the syn conformer, the equivalent interaction involves a C−H ring bond that is practically unpolarized. Using the MP2-calculated geometries and NBO charges, the interaction energy between the relevant bond dipoles in the two conformers can be approximately estimated from eq 1,[42] yielding a larger stabilization of the anti conformer compared to the syn form by ∼13 kJ mol^{-1}.

$$E = \frac{\mu_a \mu_b}{4\pi\varepsilon_0 R^3}(2\cos(\theta_a)\cos(\theta_b) - \sin(\theta_a)\sin(\theta_b)\cos(\phi)) \quad (1)$$

In eq 1, μ_a and μ_b represent the interacting bond dipoles, R is the distance between their center, θ and ϕ denote the angles between the orientations of the dipoles and the line connecting their centers and the angle between the orientation of the two dipoles, respectively, and ε_0 is the permittivity of the vacuum.

The combined result of this bond dipole interaction effect (favoring the anti conformer) with the orbital interactions discussed above (which favor the syn form) is a slightly more stable syn form (the estimated value based on this very simple approach, 2 kJ mol^{-1}, agrees fairly well with the MP2-calculated relative energy of the two conformers). As will be shown later in this article, the experimental results confirm the theoretical predictions about the relative stability of the two conformers.

Figure 3 shows the B3LYP/6-311++G(d,p)-calculated potential energy profile for interconversion between the two conformers of 3QC. The calculated energy barrier amounts to 36.2 kJ mol^{-1}, and the maximum energy structure along the path corresponds to that exhibiting the perpendicular arrangement of the aldehyde substituent in relation to the ring. The calculated barrier is practically equal to those calculated at the same level of theory for benzaldehyde (36.7 kJ mol^{-1})[23] and 3-furaldehyde (38.8 kJ mol^{-1})[24] and only slightly lower than those reported for 4-methoxybenzaldehyde and 6QC (43.1 and 43.9 kJ mol^{-1}, respectively).[20,23]

Infrared Spectrum of 3QC Isolated in Solid Argon. The only vibrational data previously reported for 3QC have been obtained by Kumru et al.[36] for the compound at room temperature. Both Raman and infrared (attenuated total reflectance (ATR) data for the neat compound in the 4000−650 cm^{-1} range and transmittance infrared spectrum for the compound in a polyethylene pellet in the 650−50 cm^{-1} range) have been measured in that study and tentatively correlated with the calculated spectra for the two conformers of 3QC.[36] In the present study, monomers of 3QC have been trapped from the gas phase in a low-temperature argon matrix, and the obtained spectrum of the matrix-isolated compound has been interpreted on the basis of the theoretically predicted spectra. As is well-known,[23−25,43] for a molecule possessing two or more low energy-conformers that are significantly populated in the gas phase and that are separated from each other by relatively high energy barriers (as is the case of 3QC), the matrix isolation technique allows one to efficiently trap in a low-temperature, solid−inert gas environment the populations of conformers corresponding to the thermal equilibrium existing in the gas prior to deposition. One can then expect to have both syn and anti conformers of 3QC populated in an Ar matrix. The infrared spectrum of such a matrix should be a superposition of the infrared spectra of both matrix-isolated forms.

The relative populations of syn and anti conformers of 3QC in the gas phase at 298.15 K (which corresponds to the temperature of the vapor of the compound immediately before matrix deposition in the performed experiments) can be roughly estimated from the MP2/6-311++G**-calculated conformers' Gibbs energies as being 64 (syn) and 36% (anti). That corresponds to a [syn]/[anti] ratio equal approximately to 2:1, and such a population ratio of the two conformers is expected to be found in low-temperature matrixes with isolated 3QC monomers.

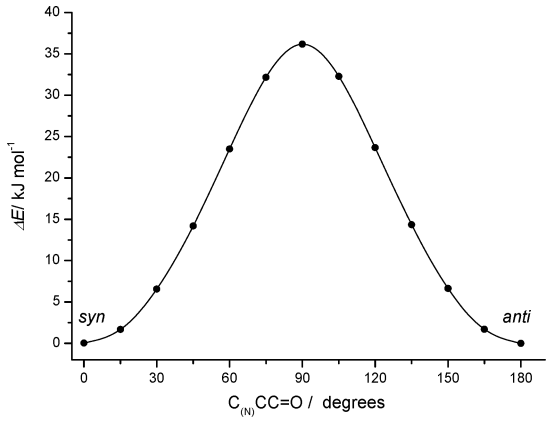

Figure 3. B3LYP/6-311++G(d,p)-calculated potential energy profile for the syn/anti conformational interconversion in 3QC.

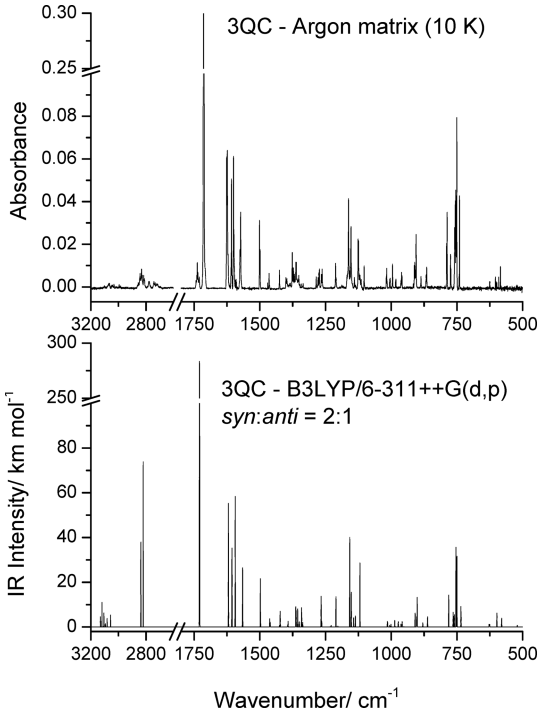

Figure 4. Infrared spectrum of 3QC isolated in an argon matrix at 10 K (top) and simulated spectrum built from the B3LYP/6-311++G(d,p)-calculated spectra for syn and anti 3QC conformers in a ratio 2:1 (bottom). In the simulated spectrum, theoretically obtained wavenumbers were scaled down by 0.978, and bands were simulated by Lorentzian functions centered at the calculated wavenumbers and with a full width at half-maximum of 1 cm^{-1}.

dx.doi.org/10.1021/jp506354t | J. Phys. Chem. A XXXX, XXX, XXX−XXX

Table 1. Observed Bands in the IR Spectrum of Matrix-Isolated 3QC, B3LYP/6-311++G(d,p)-Calculated Wavenumbers (ν), IR Intensities (I^{IR}) for the syn and anti Conformers of the Molecule, and Proposed Assignments[a]

Syn Observed	Calculated ν[b]	I^{IR}	*Anti* Observed	Calculated ν[b]	I^{IR}	Approximate Description[c]
3102	3130	7	3097	3129	8	
3069	3119	14	3068	3119	13	
3064	3105	8		3107	1	νCH rings
	3096	2	n. obs.	3104	6	
3045	3094	2		3096	0.4	
	3081	6	3031	3056	18	
2837/ 2832/ 2828	2819	119	2843/ 2817/ 2811	2836	123	ν(C–H)
1740/ 1738/ 1714/ 1712	1728	395	1736/ 1730/ 1715	1728	292	ν(C=O)
1627/ 1625/ 1624	1618	70	1625/ 1621	1619	39	
1609/ 1607/ 1605	1605	57	1599/ 1598	1593	188	
1577/ 1573	1565	39	1576/ 1573	1565	7	
1497	1497	14	1501/ 1499	1497	46	
1458	1460	3	1470/ 1464	1462	12	
1425	1422	11	n. obs.	1425	2	
1398/ 1395	1392	4	1401	1394	2	δ(C–H)
1372/ 1368	1363	15	1377/ 1372	1361	23	
1353/ 1351	1350	4	1363/ 1361	1355	26	νCC rings, δCH rings
1342/ 1336	1340	14	n.obs.	1336	7	
1278/ 1275/ 1266/ 1263	1266	22	1266	1264	8	
n. obs.	1228	1	n.obs.	1231	1	
1212/ 1209	1210	22	n. obs.	1203	1.2	
1167/ 1162/ 1161	1157	65	1158/ 1153/ 1151	1152	50	
1141/ 1140	1143	7	1125	1136	16	
1126/ 1121	1119	27	1118/ 1115	1119	41	
1019	1015	4	1018/ 1016	1013	6	
1004	1001	2	1006	1005	3	γ(C=O) (≡ γC–H)
989	983	0.2	995	986	10	
984/ 982	973	4	n. obs.	983	0.1	
961/ 959	958	4	964/ 961	963	4	
n. obs.	952	0.2	n. obs.	947	0.1	γCH rings, δ rings
905	901	21	915/ 913/ 912/ 910	909	20	
888/ 887	879	3	909/ 907	903	15	
868/ 865	862	6	867	862	3	
789/ 787	781	15	790/ 787	781	16	τ rings, δ rings
773	760	9	774	764	21	
760/ 758/ 756	754	58	754/ 753/ 752/ 751/ 750	751	48	δ(C–C=O)[d]
755/ 754/ 753/ 751	750	47	740	735	30	δ(C–C=O)[e]
626	627	1	625	627	2	
	625	2		626	1	
603	598	10	585	580	13	

[a]Wavenumber in cm^{-1}; calculated intensities in km mol^{-1}. ν, stretching; δ, bending; γ, rocking; τ, torsion. [b]Wavenumbers were scaled by 0.978. [c]In this table, only the modes assigned to the aldehyde substituent are indicated explicitly, while the vibrations associated with the rings are described in a general way; see Tables S9 and S10 (Supporting Information) for a detailed description of all vibrational coordinates. [d]In the 3QC syn conformer. [e]In the 3QC anti conformer.

Figure 4 shows the infrared spectrum recorded immediately after deposition of an argon matrix (10 K) with isolated 3QC molecules. This spectrum can be compared with the theoretical spectra of syn and anti conformers, summed with 2 and 1 weights, respectively. The full list of calculated frequencies and IR intensities as well as the results of the normal coordinate analysis (carried out for both conformers of 3QC) is provided in the Supporting Information (Tables S8–S10). The assignments of the bands observed in the experimental spectrum are given in Table 1. The assignments were made based on the results of the theoretical calculations (see Figure 4 and Tables S8–S10 (Supporting Information)) and also on the results of the performed in situ UV irradiation experiments described in detail in the next section. In those experiments, the experimental spectra of syn and anti conformers were separated thanks to the UV-induced transformation of one of the conformers into the other. As a result of such conformational interconversions, the IR bands in the spectrum belonging to one of the 3QC conformers increased in intensity, whereas the intensities of IR bands belonging to the spectrum of the other form diminished.

It is important to note here that the simulated spectrum fits very nicely the experimentally measured one. Particularly relevant in the context of the present study is the fact that the expected ratio of the conformers' populations in the gas phase prior to deposition of the matrix, estimated from the MP2-calculated energies (syn/anti ≈ 2:1), was in fact observed in the as-deposited matrix. Indeed, changing the relative contributions of the two conformers to the simulated spectrum shown in Figure 4 strongly deteriorates the agreement between this spectrum and the experimental one. Hence, the experimental results confirm the results of the calculations and show that the relative Gibbs energies of the syn and anti conformers of 3QC have been predicted very well by the MP2 calculations.

dx.doi.org/10.1021/jp506354t | J. Phys. Chem. A XXXX, XXX, XXX–XXX

Annealing of the matrix up to ~40 K was performed to check for the possibility of thermal rotamerization. However, no changes were observed in the spectrum that can be due to any conversion between the conformers, as could in fact be anticipated by taking into account the large value of the barrier for conformational isomerization (36.2 kJ mol^{-1}). The minor intensity changes observed in the spectrum upon annealing could be doubtlessly assigned to matrix−site conversion.

In Situ UV-Induced Conformational Isomerization of 3QC. The matrix-isolated 3QC was irradiated in situ using broad-band UV light produced by a Hg(Xe) lamp, combined with long-pass filters with cutoff wavelengths of 315 and 235 nm. Upon irradiation at λ > 315 nm, a redistribution of the intensities of the bands present in the IR spectrum of the original 3QC matrix was observed, while no new bands were observed (indicating that no formation of new chemical species took place upon irradiation). Figure 5 shows the difference spectrum obtained by subtracting the spectrum of the as-deposited matrix from that obtained after 100 min of irradiation at λ > 315 nm. In the figure, this spectrum is compared with the simulated theoretical difference spectrum built using the calculated spectra for the two 3QC conformers (the spectrum of the syn conformer minus the spectrum of the anti conformer). It is clear from this figure that the bands matching the predicted spectrum of the anti conformer decrease in intensity (bands pointing down in the difference experimental spectrum shown in Figure 5), while those ascribable to the syn form increase, that is, the UV irradiation of the sample at λ > 315 nm resulted in occurrence of the anti → syn conversion. Subsequent UV irradiation at shorter wavelenghts (λ > 235 nm) resulted in the reverse reaction, with repopulation of the anti conformer at the expense of the syn form (Figure 5).

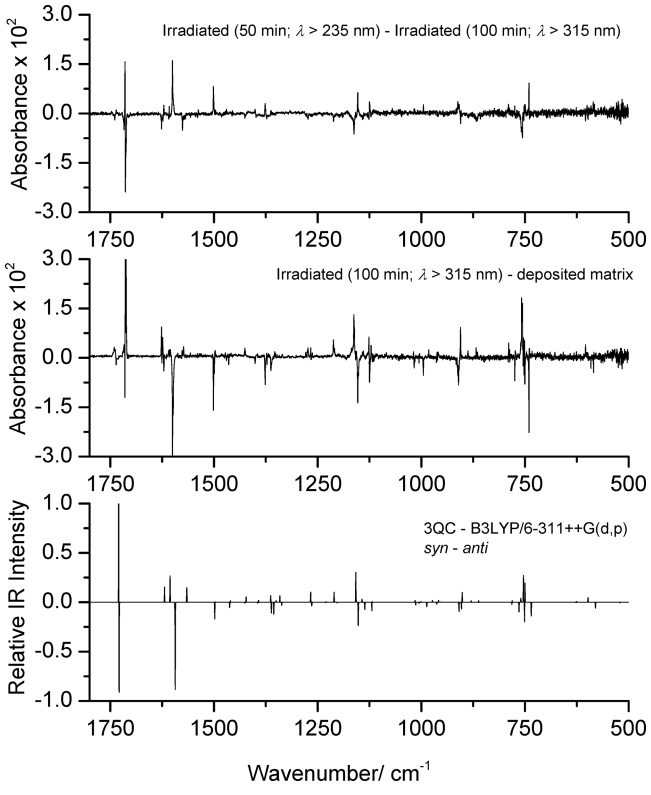

Figure 5. Infrared difference spectra of 3QC isolated in argon matrix (T = 10 K): matrix irradiated for 50 min at λ > 235 nm minus the matrix irradiated for 100 min at λ > 315 nm (top); matrix irradiated for 100 min at λ > 315 nm minus the as-deposited matrix (middle), and simulated difference spectrum built from the B3LYP/6-311++G(d,p)-calculated spectra for syn (bands pointing up) and anti (bands pointing down) 3QC conformers (bottom). In the simulated spectrum, theoretically obtained wavenumbers were scaled down by 0.978, and bands were simulated by Lorentzian functions centered at the calculated wavenumbers and with a full width at half-maximum of 1 cm^{-1}.

In an attempt to rationalize the wavelength dependence of the observed rotamerization processes (longer wavelengths favoring the anti → syn conversion; shorter wavelengths favoring the syn → anti conversion), time-dependent DFT (TD-DFT) calculations were performed [with the B3LYP functional and the 6-311++G(d,p) basis set]. The energies of vertical transitions from S_0 to the lowest-energy excited singlet states (S_1 to S_6) as well as the position of the lower triplet states (T_1 to T_6) were calculated for the syn and anti conformers of 3QC. The results of these calculations are presented in Table 2 and show that, among excitations to the S_n (n = 1, 6) states, only transition to S_2 and S_4 have substantial oscillator strengths.

Because the performed irradiation experiments were done using broad-band light, one can expect that the two conformers are being excited simultaneously (though with different efficiencies, depending on their specific absorption spectrum) and that the observed net change in the relative population of the two conformers results from the attempt of the system to attain the photostationary equilibrium characteristic for the system subjected to the selected irradiation. According to the data shown in Table 2, irradiation at λ > 315 nm shall lead predominantly to S_0 → S_2 excitation. The lower energy and higher oscillator strength for the S_0 → S_2 transition in the anti conformer of 3QC thus justified the observed anti → syn conversion when the as-deposited matrix of 3QC was irradiated with λ > 315 nm. On the other hand, the performed subsequent irradiation at higher energy can also efficiently induce other excitations (for example, the S_0 → S_4 excitation, which also has a large oscillator strength; see Table 2). This can lead to a photostationary equilibrium where the population of the anti form is increased in relation to the small population of this anti conformer, depleted by the previous irradiation at λ > 315 nm that induced the anti → syn conversion. Irradiation at λ > 235 nm then resulted in observation of the syn → anti conversion (see Figure 5).

Note also that the TD-DFT calculations also predict that several triplet states occur at energies lower than those of the S_0 → S_2 and S_0 → S_4 excitation. Intersystem crossings may then also take place after the initial excitation of the 3QC molecule, which may act either as a partial activator or as a quencher of the rotamerization processes (depending on the relative efficiencies of the new opened and closed relaxation channels), and thus leading also to a potential dependence of the position of the photostationary state between the two 3QC conformers on the excitation wavelength.

CONCLUSIONS

The structure and conformational preferences of 3-quinolinecarboxaldehyde (3QC) in the gas phase (and cryogenic argon matrix) and crystalline state were studied. In addition, the infrared spectrum and UV-induced rotamerizations for the matrix-isolated compound were investigated.

3QC was shown to crystallize in the space group $P2_1/c$ (monoclinic) with a = 6.306(4), b = 18.551(11), c = 6.999(4) Å, β = 106.111(13)°, and Z = 4. The crystals were found to

dx.doi.org/10.1021/jp506354t | J. Phys. Chem. A XXXX, XXX, XXX−XXX

Table 2. Energy of Vertical Absorptions (ΔE) and Oscillator Strengths (f) Calculated Using the TD-DET(B3LYP)/6-311++G(d,p) Method at the Ground-State Equilibrium Geometries of syn and anti Conformers of 3QC

syn				anti			
state	type	ΔE eV (nm)	f	state	type	ΔE eV (nm)	f
$S_0(A')$		–		$S_0(A')$		–	
$S_1(A')$	$\pi\pi^*$	3.47 (357)	0.0001	$S_1(A')$	$\pi\pi^*$	3.39 (366)	0.0000
$S_2(A')$	$\pi\pi^*$	3.94 (315)	0.0297	$S_2(A')$	$\pi\pi^*$	3.79 (327)	0.0312
$S_3(A'')$	$n\pi^*$	4.09 (303)	0.0010	$S_3(A'')$	$n\pi^*$	4.03 (308)	0.0010
$S_4(A')$	$\pi\pi^*$	4.23 (293)	0.0706	$S_4(A')$	$\pi\pi^*$	4.22 (294)	0.0938
$S_5(A')$	$\pi\pi^*$	4.31 (288)	0.0005	$S_5(A')$	$\pi\pi^*$	4.39 (282)	0.0004
$S_6(A'')$	$n\pi^*$	4.37 (284)	0.0001	$S_6(A'')$	$n\pi^*$	4.45 (279)	0.0001
$T_1(A')$	$\pi\pi^*$	2.74		$T_1(A')$	$\pi\pi^*$	2.60	
$T_2(A')$	$\pi\pi^*$	3.02		$T_2(A'')$	$\pi\pi^*$	2.96	
$T_3(A')$	$\pi\pi^*$	3.55		$T_3(A')$	$\pi\pi^*$	3.49	
$T_4(A'')$	$n\pi^*$	3.62		$T_4(A'')$	$n\pi^*$	3.62	
$T_5(A')$	$\pi\pi^*$	3.74		$T_5(A')$	$\pi\pi^*$	3.81	
$T_6(A')$	$\pi\pi^*$	4.15		$T_6(A')$	$\pi\pi^*$	4.13	

exhibit pseudomerohedral twinning with a twin law corresponding to a two-fold rotation around the monoclinic (100) reciprocal lattice axis (or [4 0 1] in direct space). In the crystal, 3QC molecules adopt the syn conformation.

In the gas phase, the compound exists in the syn and anti forms, in a population ratio of ~2:1 (in agreement with the MP2/6-311++G(d,p)-calculated $\Delta G°$ value of 1.44 kJ mol^{-1}), which could be successfully trapped in solid argon at 10 K.

The infrared spectrum of the matrix-isolated compound was registered and interpreted with the help of normal coordinate analysis. The assignment of the spectrum to the two 3QC conformers (syn and anti) was also facilitated by the observation of rotamerization reactions occurring upon in situ UV irradiation of matrix-isolated 3QC. UV irradiation at λ > 315 nm led to anti→syn isomerization, whereas irradiation at λ > 235 nm resulted in the syn→anti reverse phototransformation. The wavelength dependence of the observed rotamerization processes was rationalized based on the results of TD-DFT calculations. Comparison of the calculated energies and oscillator strengths of the $S_0 \rightarrow S_2$ transitions (the most important low-energy, intense transition) in the syn and anti forms of 3QC can justify the prevalence of the anti → syn conversion experimentally observed for matrixes irradiated at λ > 315 nm. Irradiation at higher energies (λ > 235 nm) can also efficiently induce other excitations and lead to a photostationary equilibrium where the population of the anti form is increased in relation to that observed in matrixes irradiated at λ > 315 nm.

■ ASSOCIATED CONTENT

Supporting Information

Tables S1–S6, with crystal data and details of the X-ray structure determination (Table S5 also presents the calculated structures for isolated syn and anti conformers of 3QC, comparing them with the structural parameters determined for the crystal of the compound); Table S7, with MP2/6-311++G(d,p)-calculated atomic NBO charges for syn and anti conformers of 3QC; Tables S8–S10, with the definition of the internal coordinates used in the normal mode analysis for 3QC and obtained results for the syn and anti conformers of 3QC; Figure S1, showing the ORTEP diagram for 3QC; and Figure S2, showing the X-ray powder diffractogram of the purchased sample of 3QC in comparison with that calculated based on the resolved single-crystal structure of the compound. This material is available free of charge via the Internet at http://pubs.acs.org.

■ AUTHOR INFORMATION

Corresponding Author

*E-mail: nkus@anadolu.edu.tr.

Notes

The authors declare no competing financial interest.

■ ACKNOWLEDGMENTS

CQC and CEMDRX are supported by the Fundação para a Ciência e a Tecnologia (FCT), Portuguese Agency for Scientific Research, through Projects PEst-OE/QUI/UI0313/2014 and PEst-OEFIS/UI0036/2014. N.K. acknowledges FCT for the award of a postdoctoral grant (SFRH/BPD/88372/2012). Access to XRD facilities of TAIL-UC funded under QREN-Mais Centro Project ICT_2009_02_012_1890 is gratefully acknowledged. The authors also thank Dr. Agnieszka Kaczor and the Academic Computer Center "Cyfronet", Krakow, Poland (Grant KBN/SGI_ORIGIN 2000/UJ/044/1999), for providing us the required computing time to undertake the most demanding calculations reported in the present work.

■ REFERENCES

(1) Runge, F. F. *Neueste Phytochemische Entdeckungen zur Begründung einer Wissenschaftlichen Phytochemie*; G. Reimer: Berlin, Germany, 1820; pp 144–159.

(2) Fron, G. Use of Bis(8-hydroxyquinolinium) Sulfate as Fungicide on Plants. *Rev. Pathol. Entomol. Veg.* **1936**, *23*, 131.

(3) Madapa, S.; Tusi, Z.; Batra, S. Advances in the Synthesis of Quinoline and Quinoline-Annulated Ring Systems. *Curr. Org. Chem.* **2008**, *12*, 1116–1183.

(4) Chen, Y. L.; Fang, K. C.; Sheu, J. Y.; Hsu, S. L.; Tzeng, C. C. Synthesis and Antibacterial Evaluation of Certain Quinolone Derivatives. *J. Med. Chem.* **2000**, *44*, 2374–2377.

(5) Vargas, L. Y.; Castelli, M. V.; Kouznetsov, V. V.; Urbina, J. M.; Lopez, S. N.; Sortino, M.; Enriz, R. D.; Ribas, J. C.; Zacchino, S. In Vitro Antifungal Activity of New Series of Homoallylamines and Related Compounds with Inhibitory Properties of the Synthesis of Fungal Cell Wall Polymers. *Bioorg. Med. Chem.* **2003**, *11*, 1531–1550.

(6) Ablordeppey, S. Y.; Fan, P.; Li, S.; Clark, A. M.; Hufford, C. D. Substituted Indoloquinolines as New Antifungal Agents. *Bioorg. Med. Chem.* **2002**, *10*, 1337–1346.

(7) Całus, S.; Gondek, E.; Danel, A.; Jarosz, B.; Pokładko, M.; Kityk, A. V. Electro-luminescence of 6-R-1,3-Diphenyl-1*H*-pyrazolo[3,4-b]quinoline-Based Organic Light-Emitting Diodes (R = F, Br, Cl, CH_3, C_2H_3 and $N(C_6H_5)_2$. *Mater. Lett.* **2007**, *61*, 3292−3295.
(8) Caeiro, G.; Lopes, J. M.; Magnoux, P.; Ayrault, P.; Ramôa Ribeiro, F. A FT-IR Study of Deactivation Phenomena in Catalytic Cracking: Nitrogen Poisoning, Coke Formation and Acidity−Activity Correlations. *J. Catal.* **2007**, *249*, 234−243.
(9) Todorovic, T. R.; Bacchi, A.; Juranic, N. O.; Sladic, D. M.; Pelizzi, G.; Bozic, T. T.; Filipovic, N. R.; Andelkovic, K. K. Synthesis and Characterization of Novel Cd(II), Zn(II) and Ni(II) Complexes with 2-Quinoline Carboxaldehyde Selenosemicarbazone. Crystal Structure of Bis(2-quinoline carboxaldehyde selenosemicarbazonato) Nickel(II). *Polyhedron* **2007**, *26*, 3428−3436.
(10) Filipovic, N. R.; Borrmann, H.; Todorovic, T. R.; Borna, M.; Spasojevic, V.; Sladic, D.; Novakovic, I.; Andjelkovic, K. K. Copper(II) Complexes of *N*-Heteroaromatic Hydrazones: Synthesis, X-ray Structure, Magnetic Behavior, and Antibacterial Activity. *Inorg. Chim. Acta* **2009**, *362*, 1996−2000.
(11) Gligorijevic, N.; Todorovic, T. R.; Radulovic, S.; Sladic, D.; Filipovic, N. R.; Godevac, D.; Jeremic, D.; Andelkovic, K. K. Synthesis and Characterization of New Pt(II) and Pd(II) Complexes with 2-Quinolinecarboxaldehyde Selenosemicarbazone: Cytotoxic Activity Evaluation of Cd(II), Zn(II), Ni(II), Pt(II) and Pd(II) Complexes with Heteroaromatic Selenosemicarbazones. *Eur. J. Med. Chem.* **2009**, *44*, 1623−1629.
(12) Sarmah, P. P.; Deb, B.; Borah, B. J.; Fuller, A. L.; Slawin, A. M. Z.; Woollins, J. D.; Dutta, D. K. Rhodium (I) Carbonyl Complexes of Quinoline Carboxaldehyde Ligands and their Catalytic Carbonylation Reaction. *J. Organomet. Chem.* **2010**, *695*, 2603−2608.
(13) Liu, Z. C.; Wang, B. D.; Yang, Z. Y.; Li, Y.; Qin, D. D.; Li, T. R. Synthesis, Crystal Structure, DNA Interaction and Antioxidant Activities of Two Novel Water-Soluble Cu^{2+} Complexes Derivated from 2-Oxo-quinoline-3-carbaldehyde Schiff-Bases. *Eur. J. Med. Chem.* **2009**, *44*, 4477−4484.
(14) Liu, Z. C.; Wang, B. D.; Li, B.; Wang, Q.; Yang, Z. Y.; Li, T. R.; Li, Y. Crystal Structures, DNA-Binding and Cytotoxic Activities Studies of Cu(II) Complexes with 2-Oxo-quinoline-3-carbaldehyde Schiff-Bases. *Eur. J. Med. Chem.* **2010**, *45*, 5353−5361.
(15) Farghally, A. M.; Habib, N. S.; Hazzaa, A. A. B.; El-Sayed, O. A. Synthesis of Substituted Quinoline-3-carbaldehyde (2,3-Dihydrothiazol-2-ylidene) Hydrazones of Potential Antimicrobial Activity. *J. Pharm. Belg.* **1985**, *40*, 366−372.
(16) Kombarov, P. V.; Yurovskaya, M. A. 2-Chloro-3-quinolinecarboxaldehyde in the Synthesis of Condensed Quinoline Systems. 1. Synthesis of Derivatives of 3,4-Dihydro-2*H*-[1,3]thiazino[6,5-b]-quinolines. *Chem. Heterocycl. Compd.* **2003**, *39*, 364−367.
(17) Maria, T. M. R.; Eusébio, M. E. S.; Silva, J. A.; Sobral, A. J. F. N.; Cardoso, C.; Paixão, J. A.; Silva, M. R. 2-Quinolinecarboxaldehyde: Polymorphic Behavior of a Small Rigid Molecule. *J. Mol. Struct.* **2012**, *1030*, 67−74.
(18) Motswainyana, W. M.; Onani, M. O. Quinoline-2-carbaldehyde. *Acta Crystallogr., Sect. E* **2011**, *67*, o2573.
(19) Küçük, V.; Altun, A.; Kumru, M. Combined Experimental and Theoretical Studies on the Vibrational Spectra of 2-Quinolinecarboxaldehyde. *Spectrochim. Acta, Part A* **2012**, *85*, 92−98.
(20) Kumru, M.; Küçük, V.; Kocademir, M. Determination of Structural and Vibrational Properties of 6-Quinolinecarboxaldehyde Using FT-IR, FT-Raman and Dispersive-Raman Experimental Techniques and Theoretical HF and DFT (B3LYP) Methods. *Spectrochim. Acta, Part A* **2012**, *96*, 242−251.
(21) Khan, F. N.; Subashini, R.; Kumar, R.; Hathwar, V. R.; Ng, S. W. 2-Chloro-6-methylquinoline-3-carbaldehyde. *Acta Crystallogr., Sect. E* **2009**, *65*, o2710.
(22) Rosenberg, E.; Rokhsana, D.; Nervi, C.; Gobetto, R.; Milone, L.; Viale, A.; Fiedler, J.; Botavina, M. A. Synthesis, Reduction Chemistry, and Spectroscopic and Computational Studies of Isomeric Quinolinecarboxaldehyde Triosmium Clusters. *Organometallics* **2004**, *23*, 215−223.
(23) Kuş, N.; Sharma, A.; Reva, I.; Lapinski, L.; Fausto, R. Thermal and Photoinduced Control of Relative Populations of 4-Methoxybenzaldehyde (*p*-Anisaldehyde) Conformers. *J. Phys. Chem. A* **2010**, *114*, 7716−7724.
(24) Kuş, N.; Reva, I.; Fausto, R. Photoisomerization and Photochemistry of Matrix-Isolated 3-Furaldehyde. *J. Phys. Chem. A* **2010**, *114*, 12427−12436.
(25) Giuliano, B. M.; Reva, I.; Fausto, R. Infrared Spectra and Photochemistry of Matrix-Isolated Pyrrole-2-carbaldehyde. *J. Phys,. Chem. A* **2010**, *114*, 2506−2517.
(26) Frisch, M. J.; Trucks, G. W.; Schlegel, H. B.; Scuseria, G. E.; Robb, M. A.; Cheeseman, J. R.; Scalmani, G.; Barone, V.; Mennucci, B.; Petersson, G. A.; et al. *Gaussian 09*, revision A.02; Gaussian, Inc.: Wallingford, CT, 2009.
(27) McLean, A. D.; Chandler, G. S. Contracted Gaussian-Basis Sets for Molecular Calculations. 1. 2nd Row Atoms, Z=11−18. *J. Chem. Phys.* **1980**, *72*, 5639.
(28) Becke, A. D. Density-Functional Exchange-Energy Approximation with Correct Asymptotic Behavior. *Phys. Rev. A* **1988**, *38*, 3098−3100.
(29) Lee, C. T.; Yang, W. T.; Parr, R. G. Development of the Colle−Salvetti Correlation Energy Formula into a Functional of Electron Density. *Phys. Rev. B* **1988**, *37*, 785−789.
(30) Vosko, S. H.; Wilk, L.; Nusair, M. Accurate Spin-Dependent Electron Liquid Correlation Energies for Local Spin Density Calculations: A Critical Analysis. *Can. J. Phys.* **1980**, *58*, 1200−1211.
(31) Schachtschneider, J. H.; Mortimer, F. S. *Vibrational Analysis of Polyatomic Molecules. VI. FORTRAN IV Programs for Solving the Vibrational Secular Equation and for the Least-Squares Refinement of Force Constants, Project No. 31450. Structural Interpretation of Spectra*; Shell Development Co.: Houston, TX, 1969.
(32) Weinhold, F.; Landis, C. R. Valency and Bonding. *A Natural Bond Orbital Donor−Acceptor Perspective*; Cambridge University Press: New York, 2005.
(33) Reed, A. E.; Curtiss, V.; Weinhold, F. Intermolecular Interactions from a Natural Bond Orbital, Donor−Acceptor Viewpoint. *Chem. Rev.* **1988**, *88*, 899−926.
(34) Bauernschmitt, R.; Ahlrichs, R. Treatment of Electronic Excitations Within the Adiabatic Approximation of Time Dependent Density Functional Theory. *Chem. Phys. Lett.* **1996**, *256*, 454−464.
(35) Stratmann, R. E.; Scuseria, G. E.; Frisch, M. J. An Efficient Implementation of Time-Dependent Density-Functional Theory for the Calculation of Excitation Energies of Large Molecules. *J. Chem. Phys.* **1998**, *109*, 8218−8224.
(36) Kumru, M.; Küçük, V.; Bardakçı, T. Theoretical and Experimental Studies on the Vibrational Spectra of 3-Quinolinecarboxaldehyde. *Spectrochim. Acta, Part A* **2012**, *90*, 28−34.
(37) Kulbida, A.; Ramos, M. N.; Räsänen, M.; Nieminen, J.; Schrems, O.; Fausto, R. Rotational Isomerism in Acrylic Acid: A Combined Matrix-Isolated Infrared, Raman and *Ab Initio* Molecular Orbital Study. *J. Chem. Soc., Faraday Trans. 2* **1995**, *91*, 1571−1585.
(38) Fausto, R.; Kulbida, A.; Schrems, O. UV-Induced Isomerization of (E)-crotonic Acid: A Combined Matrix-Isolated Infrared and Ab Initio Molecular Orbital Study. *J. Chem. Soc., Faraday Trans. 2* **1995**, *91*, 3755−3770.
(39) Fausto, R.; Batista de Carvalho, L. A. E.; Teixeira-Dias, J. J. C.; Ramos, M. N. The *s-cis* and *s-trans* Conformers of Formic, Thioformic and Dithioformic Acids: An Ab Initio Study. *J. Chem. Soc., Faraday Trans. 2* **1989**, *85*, 1945−1962.
(40) McKean, D. C. Individual CH Bond Strengths in Simple Organic Compounds: Effects of Conformation and Substitution. *Chem. Soc. Rev.* **1978**, *7*, 399−422.
(41) Castiglioni, C.; Gussoni, M.; Zerbi, G. Intramolecular Electrical and Dynamical Interactions in Formaldelyde. A Discussion Based on Infrared Intensity Data. *J. Chem. Phys.* **1985**, *82*, 3534−3541.
(42) Atkins, P. W.; De Paula, J. *Physical Chemistry*, 8th ed.; W. H. Freeman and Company, New York, 2006; Chapter 18.
(43) Reva, I. D.; Stepanian, S. G.; Adamowicz, L.; Fausto, R. Missing Conformers: Comparative Study of Conformational Cooling in

Cyanoacetic Acid and Methyl Cyanoacetate Isolated in Low Temperature Inert Gas Matrixes. *Chem. Phys. Lett.* **2003**, *374*, 631−638.

dx.doi.org/10.1021/jp506354t | *J. Phys. Chem. A* XXXX, XXX, XXX−XXX